Available online www.jsaer.com

***Journal of Scientific and Engineering Research*, 2020, 7(6):98-103**

Research Article

ISSN: 2394-2630
CODEN(USA): JSERBR

Development of Inhomogeneous Femoral Bone Model for CT-Based Finite Element Analysis

Nor Aiman Nor Izmin[1], Fatin Hazwani[2], Mitsugu Todo[3], Abdul Halim Abdullah[1,*]

[1]Faculty of Mechanical Engineering, UniversitiTeknologi MARA (UiTM), 40450 Shah Alam, Selangor Malaysia
[2]Interdiciplinary Graduate School of Engineering Sciences, Kyushu University, 6-1 Kasuga-koen, Kasuga 816-8580, Japan
[3]Research Institute for Applied Mechanics, Kyushu University, 6-1 Kasuga-koen, Kasuga 816-8580, Japan
*Email: halim471@uitm.edu.my

Abstract Computational analysis is widely used in biomechanical analysis to predict the performance of joint replacement and bone behaviors. The non-geometrical and inhomogenous model of the bone become a big challenge in developing the 3D model. In this study, development of the 3D femoral bone model was conducted from CT-images of osteoarthritis patient using commercial biomedical software. The CT images presenting a 47 years old patient with body mass index (BMI) of 30.3. Four stages involved in this study which (i) to extract the CT image into the software, (ii) refinement of the 3D bone model, (iii) applying the loading and boundary conditions, and (iv) results and findings. The assignment of the inhomogeneous bone model was generated based on the linear relationship between gray scales area and the 'apparent density' of the CT image. Loading of 238 % of human body weight will be exerted to the femoral bone head as the hip contact force, and 104% of abductor muscle force to present the normal walking activity. Results show that the 3D model of inhomogeneous femoral bone was successfully developed from the CT-images. Variation of young modulus and bone mineral density indicated different stiffness of the cortical and cancellous bone at each particular element.

Keywords CT-based images, Inhomogeneous model, Finite Element Analysis, Convergence study

Introduction

Finite Element Analysis is widely used and one of the most reliable method in biomechanical analysis especially in predicting the performance of joint replacements [1,2] and bone behaviors [3]. Stress-strain distribution and displacements are examples of basic findings and measurement to be related to bone adaptation, resorptions and micromotions [4,5]. Various boundary and loading conditions can be simulated by using FEM compared to experimental analysis. Customized loading assignment within the model contribute to the mimic of physiological loading and further encourage the accuracy of the analysis [7]. However, the biggest challenges in the computational analysis is to model the unique, non-geometrical and inhomogeneous model of the bone [4]. Early 2000s, researchers were using 3D scanning to get the non-geometrical model of the bone from sawbones [8,9] and extract the data from CT-based images to reconstruct the 3D bone model. In this study, development of the 3D femoral bone model was conducted from CT-images of osteoarthritis patient. The CT-images was extract in commercial biomedical software namely Mechanical Finder v10 to construct the non-geometrical and inhomogeneous femoral bone model.

Material & Methods

Development of Inhomogeneous model from CT-images

The computed tomography (CT) based image data acquired from the Teijin Nakashima Medical Co. Ltd. was in the standard DICOM format. The purpose of using the CT image is because of its availability to construct the 3D model of the femoral bone by revealing the anatomic details of the internal organ which are not visible by using the conventional X-ray. The images will be appeared in slices according to the scanning area of the patient's body part. The CT image provided represent a 47 years old patient with body mass index (BMI) of 30.3. The data represent hip osteoarthritis patient on the left femur. Several phases need to be done before the result and analysis from the simulation could be retrieved. Those phases were categorized into four (4) stages. The first stage is to extract the CT image into the Mechanical Finder software. The second stage is the refinement of the 3D bone model based on the patient's CT image. The third stage before obtaining the results is by applying the loading and boundary conditions to represent a normal walking condition.

In this study, the CT images acquired were on the bones at the lower limb section as shown in Figure 1(a) before the images of the undesired bone parts being eliminated. Each slice of the CT image contains the region of interest (ROI) of the bone area. The desired bone area was selected until it forms the perfect shape of the bone structure which in this case was the femoral bone. This phase was known as shape forming and at the end stage of this first phase, an isometric view of the selected bone part was seen. The 3D femoral bone model will be seen after performing the selection of the femoral bone area in the ROI extraction phase. The 3D femoral bone model emerged when the selected area throughout the images range being stacked together vertically as shown in Figure 1(b) and (c).

(a) 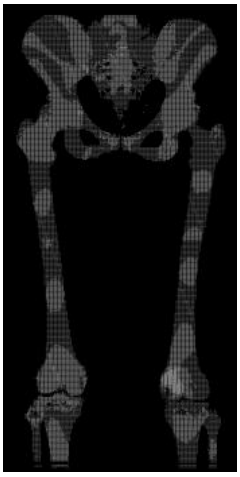 *(b)* 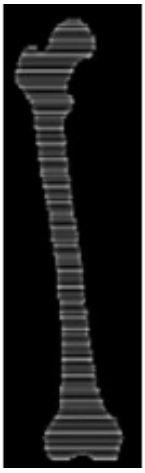 *(c)* 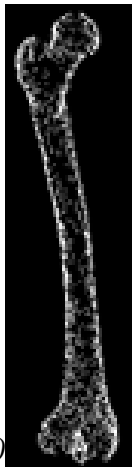

Figure 1: CT-images of (a) a lower limb, (b) vertical stack of femoral bone, and (c) Extraction for3D femoral bone model

The assignment of the inhomogeneous bone model was generated based on the linear relationship between gray scales area and the 'apparent density' of the CT image (in Hounsfield unit, HU). The solid element in the bone model was based on the CT value before calculating the density. Calculation of the bone density for each element will develop the variation of young's modulus and bone mineral density of the femoral bone model. The correlation was predicted based on previous report by Keyak *et al* [10]. Table1 shows the estimation of young's modulus and yield stress of the model based on the bone density range.

Table 1: Calculation for young's modulus and yield strength of the femoral bone model [10]

Density range	Young Modulus (MPa)
$\rho = 0$	$E = 0.001$
$0 < \rho \leq 0.27$	$E = 33900\rho^{2.20}$
$0.27 < \rho < 0.6$	$E = 5307\rho+469$
$0.6 \leq \rho$	$E = 10200\rho^{2.01}$
$\rho = 0$	$E = 0.001$

Density range	Yield strength (MPa)
$\rho \leq 0.2$	$\sigma_r=1.0 \times 10^{20}$
$0.2 < \rho < 0.317$	$\sigma_r= 137\ \rho^{1.88}$
$0.317 \leq \rho$	$\sigma_r= 114\ \rho^{1.72}$

Loading & Boundary Condition

The loading and boundary conditions applied in this study are based on experimental study conducted by Bergmann et al. [11]. About 238 % of human body weight will be exerted to the femoral bone head as the hip contact force, and 104% of abductor muscle force [12] during normal walking activity. Thus, the load magnitude and direction were applied according to both studies, which acted at the femoral bone head for the hip contact force and the greater trochanter of the femoral bone as the abductor muscle force.

Convergence Study

The convergence study has been conducted by selecting seven (7) mesh sizes which were from 2 mm to 8 mm of linear tetrahedral elements. A simple mechanical analysis has been conducted to all femur models with a 1000 N distributed load applied on top of the femoral head. The load value and direction applied for this convergence study were similar for all 7 models. Figure 2 (a) - (g) shows the example of half femur with mesh sizes from 2mm until 8mm respectively.

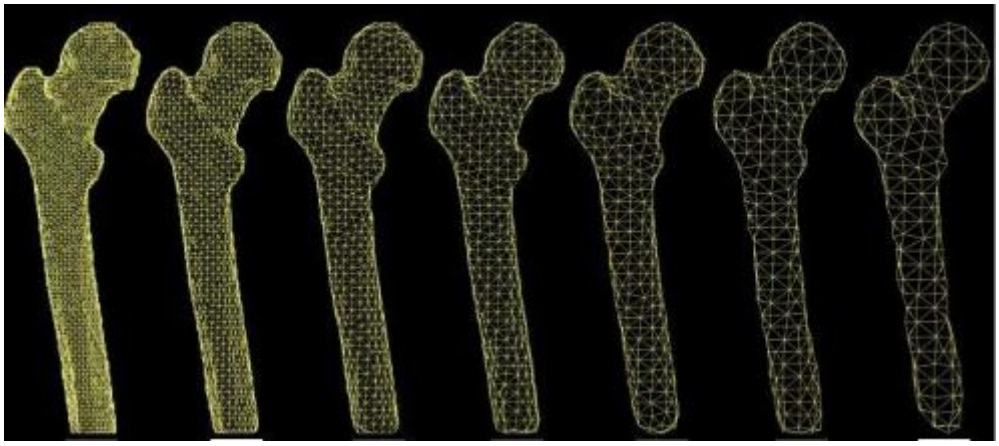

(a) (b) (c) (d) (e) (f) (g)

Figure 2: Different mesh size of the femoral bone for convergence study (a)2mm, (b) 3mm, (c) 4mm, (d) 5mm, (e)6mm, (f) 7mm and (g) 8mm

Results & Discussion

Inhomogeneous model of femoral bone

The variation of the young modulus and bone mineral density of the inhomegeneous femoral bone was illustrated in Figure 3(a) and (b), respectively.

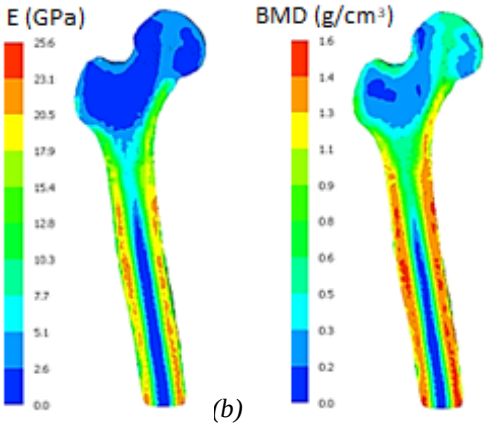

(a) (b)

Figure 3: Variation of (a) young modulus and (b) bone mineral density, BMD for femoral bone model

The stiffer material with higher value of young modulus and bone mineral density represents the cortical bone (outer part) while the lower value in the middle region represents the cancellous bone. The femoral shaft indicate higher value of young's modulus and BMD distribution, compared to the proximal area of the femur. The inhomogeneous model was closely identical to real femoral bone as the development of the model was adapted based on the HU unit of CT-images [10,13]. Cortical bone experienced higher stiffness while cancellous spone react as spongy materials.

The inhomogeneous bone model in this research was validated with the experimental study conducted by Simoes et al. [14]. In this research, the validation of the strain distribution was done by using the intact femur model. A simulation analysis has been conducted which referred to the author's second load case since it is similar to the loading and boundary condition applied in this research. The load applied for the joint reaction force and abductor muscle force in this results validation section were700 N and 300 N respectively with a fixed boundary at the end of the femur as conducted by the experimental study [14]. The result of the microstrain distribution as shown in Figure 4 was extracted based on the medial and lateral aspects which further verified with experimental study as reported by Simoes et al [14]. The similar pattern of the strain distribution between both study suggested the verification of the inhomogeneous model conducted in this study [13,15]. Different magnitude appeared in both study might be due to different bone models in the study.

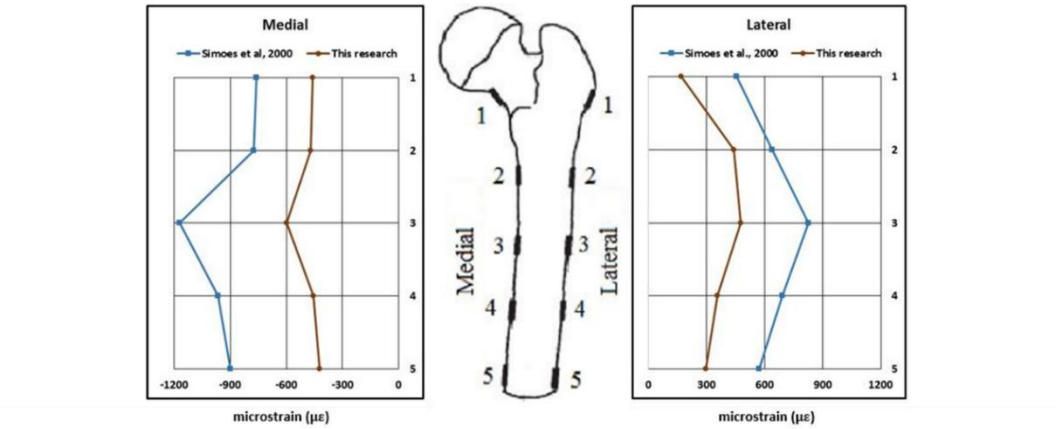

Figure 4:Verification of the inhomogeneous femoral model with previous study

Convergence analysis for meshing sizes

Based on the findings in the convergence study, the mechanical analysis results(Figure 5) of the bone displacement and maximum stress show a converged value from(a) 2 mm until (d) 5 mm; thus, 5 mm mesh size was selected to be used in this study. The number of nodes and triangles generated on the selected mesh size of the femoral bone model was 846 and 1688 respectively. Smaller size of meshing is expected to give similar findings and only consume more computational time.

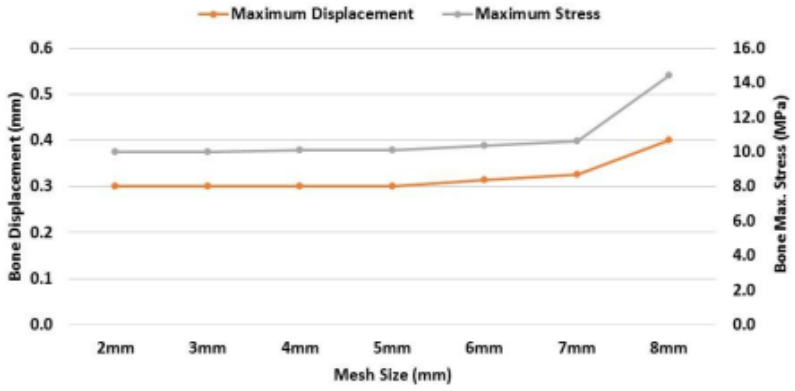

Figure 5:Maximum equivalent stress and displacement in femoral bone model for convergence study

Drucker-Prager Stress Distribution

The stress distribution of the femoral bone for normal walking activity is presented in Figure 6. Higher stress is predicted at the middle area of medial and lateral region due to bending effects after loaded. Then, the stress is reduced gradually until the distal end of the femur. Femoral shaft dominates most of the stress as compare to proximal region. This phenomenon is parallel to the higher young modulus and bone mineral density of the bone as indicated earlier. The higher stress to the bone contribute to stiffness of the bone.

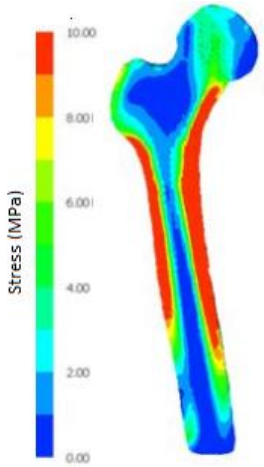

Figure 6:Drucker-Prager equivalent stress of femoral bone at normal walking activity

Conclusion

The 3D model of inhomogeneous femoral bone was successfully developed from CT-images. Variation of young modulus and bone mineral density indicated different stiffness of the cortical and cancellous bone. The computational findings are verified to experimental study conducted by previous researcher. Convergence study suggested the meshing size of 5mm for the analysis. Finite element analysis conducted show the stress distribution along the femur at the normal walking activity.

Acknowledgment

This research was supported by Universiti Teknologi MARA, UiTM under Grant No. 600-IRMI/PERDANA 5/3 BESTARI (103/2018). We thank and acknowledge the Ministry of Higher Education, Malaysia, and our colleagues from the Teijin Nakashima Medical Co. Ltd. who provided insight and expertise in the research work.

References

1. Shuib, S., Sahari, B. B., Voon, W. S., & Arumugam, M. (2012). Finite Elemental Analysis of Outer and Inner Surfaces of The Proximal Half of An Intact Femur. *Trends in Biomaterials and Artificial Organs*, 26(2), 103–106.
2. Marwan S. H., Tardan, G., Zainal, M. S.,& Abdullah, A. H. (2017). Effects of Stem Mal-alignment in The Primary Stability of Total Hip Arthroplasty. *Journal of Mechanical Engineering*, 4(4), 79-91.
3. Watanabe, Y., Shiba, N., Matsuo, S., Higuchi, F., Tagawa, Y., & Inoue, A. (2000) Biomechanical study of the resurfacing hip arthroplasty. Finite element analysis of the femoral component. *Journal of Arthroplasty*,15(4), 505–511.
4. Bessho, M., Ohnishi, I., Matsuyama, J., Matsumoto, T., Imai, K., & Nakamura, K. (2007) Prediction of strength and strain of the proximal femur by a CT-based finite element method. *Journal of Biomechanics*, 40, 1745–1753.
5. Jeon, I., Bae, J.Y., Park, J.H., Yoon, T.R., Todo, M., Mawatari, M., & Hotokebuchi, T. (2011) The biomechanical effect of the collar of a femoral stem on total hip arthroplasty. *Computer Methods Biomechanics and Biomedical Engineering*, 14(1), 103–112.

6. Abe, H., Sakai, T., Takao, M., Nishii, T., Nakamura, N. & Sugano, N. (2015). Difference in Stem Alignment Between the Direct Anterior Approach and the Posterolateral Approach in Total Hip Arthroplasty. *Journal of Arthroplasty*, 30(10), 1761–1766.
7. Little, J.P., Viceconti, T., Murray, D. W., & Gill, H.S. (2007). Changes in femur stress after hip resurfacing arthroplasty: response to physiological loads. *Clinical Biomechanics*, 22, 440–448.
8. Schmutz, B., Reynolds, K. J., & Slavotinek, J.P. (2006). Development and Validation of a Generic 3D Model of the Distal Femur, *Computer Methods in Biomechanics and Biomedical Engineering*, 9(5), 305-312.
9. Laporte, S., Skalli, W., de Guise, J. A., Lavaste, F., & Mitton, D. (2003). A Biplanar Reconstruction Method Based on 2D and 3D Contours: Application to the Distal Femur, *Computer Methods in Biomechanics and Biomedical Engineering*, 6(1), 1-6.
10. Keyak, J. H., Rossi, S. A., Jones, K. A., & Skinner, H. B. (1997). Prediction of femoral fracture load using automated finite element modeling. *Journal of Biomechanics*, 31(2), 125–133.
11. Bergmann, G., Deuretzbacher, G., Heller, M., Graichen, F., Rohlmann, A., Strauss, J., & Duda, G. N. (2001). Hip contact forces and gait patterns from routine activities. *Journal of Biomechanics*, 34(7), 859–871.
12. Heller, M. O., Bergmann, G., Kassi, J. P., Claes, L., Haas, N. P. & Duda, G. N. (2005). Determination of muscle loading at the hip joint for use in pre-clinical testing. *Journal of Biomechanics*, 38(5), 1155–1163.
13. Abdullah, A. H., Todo, M., & Nakashima Y. (2017). Prediction of damage formation in hip arthroplasties by finite element analysis using computed tomography images. *Medical Engineering & Physics*, 44, 8–15.
14. Simões, J. A., Vaz, M. A., Blatcher, S., & Taylor, M. (2000). Influence of head constraint and muscle forces on the strain distribution within the intact femur. *Medical Engineering & Physics*, 22(7), 453–459.
15. Soodmand, E., Kluess, D., Varady, P. A., Cichon, R., Schwarze, M., Gehweiler, D., Niemeyer, F., Pahr, D., & Woiczinski, M. (2018). Interlaboratory comparison of femur surface reconstruction from CT data compared to reference optical 3D scan, *BioMedical Engineering OnLine*, 17, 29.